

# Electro-optic coupling of wide wavelength range in linear chirped-periodically poled lithium niobate and its applications

Xiao-qi Zeng, Li-xiang Chen, Hai-bo Tang, Bing-zhi Zhang, Dong-zhou Zhong, and Wei-long She\*

State Key Laboratory of Optoelectronic Materials and Technologies, Sun Yat-sen University, Guangzhou 510275, China

\*shewl@mail.sysu.edu.cn

**Abstract:** We theoretically investigate the electro-optic coupling in an optical superlattice of linear chirped-periodically poled lithium niobate. It is found that the electro-optic coupling in such optical superlattice can work in a wide wavelength range. Some of examples, with bandwidths of 20, 40, 80, 120nm, are demonstrated. The way to determine the electric field for perfect conversion between o- and e-ray and the method using apodized crystals of tanh profile to reduce the ripples are shown. As one of its applications, one kind of broadband Solc-type bandpass filter in optical communication range is proposed.

©2010 Optical Society of America

**OCIS codes:** (190.0190) Nonlinear optics; (230.2090) Electro-optical devices; (120.2440) Filters.

---

## References and links

1. Y. Y. Zhu, and N. B. Ming, "Dielectric super-lattices for nonlinear optical effects," *Opt. Quantum Electron.* **31**(11), 1093–1128 (1999).
2. K. L. Baker, "Single-pass gain in a chirped quasi-phase-matched optical parametric oscillator," *Appl. Phys. Lett.* **82**(22), 3841–3843 (2003).
3. L. Arizmendi, "Photonic applications of Lithium Niobate," *Phys. Status Solidi A* **201**(2), 253–283 (2004).
4. Y. Q. Lu, Z. L. Wan, Q. Wang, Y. X. Xi, and N. B. Ming, "Electro-optic effect of periodically poled optical superlattice LiNbO<sub>3</sub> and its applications," *Appl. Phys. Lett.* **77**(23), 3719–3721 (2000).
5. C. S. Kee, Y. L. Lee, and J. Lee, "Electro- and thermo-optic effects on multi-wavelength Solc filters based on  $x^{(2)}$  nonlinear quasi-periodic photonic crystals," *Opt. Express* **16**(9), 6098–6103 (2008).
6. X. Chen, J. Shi, Y. Chen, Y. Zhu, Y. Xia, and Y. Chen, "Electro-optic Solc-type wavelength filter in periodically poled lithium niobate," *Opt. Lett.* **28**(21), 2115–2117 (2003).
7. Y. H. Chen, and Y. C. Huang, "Actively Q-switched Nd:YVO<sub>4</sub> laser using an electro-optic periodically poled lithium niobate crystal as a laser Q-switch," *Opt. Lett.* **28**(16), 1460–1462 (2003).
8. M. Charbonneau-Lefort, M. M. Fejer, and B. Afeyan, "Tandem chirped quasi-phase-matching grating optical parametric amplifier design for simultaneous group delay and gain control," *Opt. Lett.* **30**(6), 634–636 (2005).
9. M. B. Nasr, S. Carrasco, B. E. Saleh, A. V. Sergienko, M. C. Teich, J. P. Torres, L. Torner, D. S. Hum, and M. M. Fejer, "Ultrabroadband biphotons generated via chirped quasi-phase-matched optical parametric down-conversion," *Phys. Rev. Lett.* **100**(18), 183601 (2008).
10. H. Suchowski, D. Oron, A. Arie, and Y. Silberberg, "Geometrical representation of sum frequency generation and adiabatic frequency conversion," *Phys. Rev. A* **78**(6), 063821 (2008).
11. H. Suchowski, V. Prabhudesai, D. Oron, A. Arie, and Y. Silberberg, "Robust adiabatic sum frequency conversion," *Opt. Express* **17**(15), 12731–12740 (2009).
12. R. L. Sutherland, *Handbook of Nonlinear Optics*, 2nd ed. (Marcel Dekker, 2003), Chap. 17.
13. C. H. von Helmolt, "Broadband single-mode TE/TM converters in LiNbO<sub>3</sub>: a novel design," *Electron. Lett.* **22**(3), 155–156 (1986).
14. O. Eknoyan, W. K. Burns, R. P. Moeller, and N. J. Frigo, "Broadband LiTaO<sub>3</sub> guided-wave TE-TM mode converter," *Appl. Opt.* **27**(1), 114–117 (1988).
15. W. L. She, and W. K. Lee, "Wave coupling theory of linear electrooptic effect," *Opt. Commun.* **195**(1-4), 303–311 (2001).
16. G. Zheng, H. Wang, and W. She, "Wave coupling theory of Quasi-Phase-Matched linear electro-optic effect," *Opt. Express* **14**(12), 5535–5540 (2006).
17. L. D. Landau, "Zur Theorie der Energieübertragung. II," *Phys. Soviet Union* **2**, 46–51 (1932).
18. C. Zener, "Non-adiabatic Crossing of Energy Levels," *Proc. R. Soc. Lond., A Contain. Pap. Math. Phys. Character* **137**(833), 696–702 (1932).

19. M. V. Hobden, and J. Warner, "The temperature dependence of the refractive indices of pure lithium niobate," *Phys. Lett.* **22**(3), 243–244 (1966).
20. Optoplex support, "DWDM ITU Grid Specification," (Optoplex corporation,2010), <http://www.optoplex.com/PDF/DWDM-ITU.pdf>.
21. J. Huang, X. P. Xie, C. Langrock, R. V. Roussev, D. S. Hum, and M. M. Fejer, "Amplitude modulation and apodization of quasiphasematched interactions," *Opt. Lett.* **31**(5), 604–606 (2006).
22. T. Umeki, M. Asobe, Y. Nishida, O. Tadanaga, K. Magari, T. Yanagawa, and H. Suzuki, "Widely tunable 3.4  $\mu\text{m}$  band difference frequency generation using apodized  $\chi^{(2)}$  grating," *Opt. Lett.* **32**(9), 1129–1131 (2007).
23. Y. L. Lee, Y. C. Noh, C. S. Kee, N. E. Yu, W. Shin, C. Jung, D. K. Ko, and J. Lee, "Bandwidth control of a Ti:PPLN Solc filter by a temperature-gradient-control technique," *Opt. Express* **16**(18), 13699–13706 (2008).

## 1. Introduction

In recent years, many kinds of one-dimensional dielectric optical superlattices [1,2] have been widely used in the field of nonlinear optics for their beautiful function of quasi-phase matching (QPM). And among them, those made of lithium niobate ( $\text{LiNbO}_3$ ) have attracted much attention due to the large nonlinear coefficients [3]. Quasi-phase matched electro-optic coupling in periodically poled  $\text{LiNbO}_3$  (PPLN) [4], quasi-periodically poled  $\text{LiNbO}_3$  [5] and some of applications, such as Solc-type filters [5,6] and Q-switch [7] have been reported both theoretically and experimentally. As well known, the QPM in periodic or quasi-periodic optical superlattices is sensitive to the wavelength of light. However, it was found that in chirped-periodic optical superlattice, the nonlinear optical processes based on QPM [2,8–11] can be realized in a broad wavelength range.

On the other hand, the electro-optic effect has been widely used in electro-optic polarization converters as well as filters [12]. For some particular uses, for example, the polarization conversion of broadband continuous-wave [13,14] or ultrafast laser pulses, the electro-optic coupling with a function of broadband and selected wavelength range is desired. To realize the function, some special phase matching techniques [13,14] have been proposed. However, the structure and operation of such devices are quite complex and the bandwidth of them is still restricted. In this paper, we report the electro-optic coupling of wide wavelength range with a high coupling efficiency in a linear chirped-periodically poled  $\text{LiNbO}_3$  (LCPLN). The QPM design of this kind of device would be useful for broad wavelength range electro-optic polarization converters or bandpass filters.

## 2. Theory

Linear electro-optic effect, as one kind of second order nonlinear optical effects, has been shown to be able to be described by wave coupling theory [15]. Now we consider a LCPLN poled along  $z$ -axis with a monochromatic light propagating along  $x$ -axis and an electric field applied along  $y$ -axis. According to Ref [16], the electro-optic wave coupling of ordinary-ray (o-ray) and extraordinary-ray (e-ray) in a LCPLN can be described by the following equations:

$$\frac{d}{dx} A_1(x) = -i\kappa(x) A_2(x) \exp[i\varphi(x)] - iv(x) A_1(x), \quad (1a)$$

$$\frac{d}{dx} A_2(x) = -i\kappa^*(x) A_1(x) \exp[-i\varphi(x)]. \quad (1b)$$

where  $\kappa(x) = \frac{\pi}{\lambda_0} (n_o n_e)^{3/2} r_{51} E_y f_1(x)$ ,  $v(x) = \frac{\pi}{\lambda_0} n_o^3 r_{22} E_y f_0(x)$ ,  $\varphi(x) = \int_0^x \Delta k'(u) du$ ,

$\Delta k'(x) = \Delta k(\lambda_0) + K_1(x)$ ,  $\Delta k(\lambda_0) = \frac{2\pi}{\lambda_0} (n_e - n_o)$ ,  $K_1(x) = \frac{2\pi}{\Lambda(x)} = K_0 - \alpha x$ , and  $\kappa^*(x)$

denotes the complex conjugate of  $\kappa(x)$ .  $A_j(x)$  ( $j = 1, 2$ ) are the complex amplitudes corresponding to o- and e-ray, respectively;  $\lambda_0$  is the vacuum wavelength of incident light;

$n_o$  and  $n_e$  are the refractive indices of o-ray and e-ray, respectively;  $r_{51}$  and  $r_{22}$  are the linear electro-optic coefficients of LiNbO<sub>3</sub>;  $E_y$  is the applied electric field along y-axis;  $\Delta k(\lambda_0)$  denotes the wave-vector mismatch. In a LCPLN,  $K_1(x)$  is the first order reciprocal vector, where  $K_0$  is the reciprocal vector at  $x = 0$  and  $\alpha$  is a constant called chirp coefficient. When  $\Delta k(x_{pm}) = 0$ , perfect QPM is reached. Here,  $x_{pm}$  is called perfect phase matching point of  $\lambda_0$ .

We now first consider a LCPLN of length  $L$ , with a duty cycle of 0.5,  $f_1(x) = 2/(i\pi)$  and  $f_0(x) = 0$ ,  $\kappa(x) = \kappa = 2(n_o n_e)^{3/2} r_{51} E_y / (i\lambda_0)$ ,  $v(x) = 0$ . The reciprocal vector  $K_1(x) = K_0 - \alpha x$  varies continuously from  $K_0$  to  $K_0 - \alpha L$ . And the wave-vector mismatch between o-and e-ray is  $\Delta k(\lambda_0) = 2\pi(n_e - n_o) / \lambda_0$ . So the wavelength range, in which QPM can be satisfied, is approximatively from  $\lambda_1$  to  $\lambda_2$  ( $\lambda_2 > \lambda_1$ ) with its center at  $\lambda_{0.5}$ , where  $\lambda_{0.5}$  is the wavelength whose perfect phase matching point is at  $x_{pm} = 0.5L$ . Here,

$$\lambda_1 = \frac{2\pi}{K_0}(n_{o1} - n_{e1}), \quad \lambda_2 = \frac{2\pi}{K_0 - \alpha L}(n_{o2} - n_{e2}), \quad \lambda_{0.5} = \frac{2\pi}{K_0 - 0.5\alpha L}(n_o - n_e). \quad (2)$$

Since  $\alpha L$  is usually much smaller than  $K_0$ ,  $\lambda_1 \approx \lambda_{0.5}(1 - 0.5\alpha L\lambda_{0.5}/K_0)$ ,  $\lambda_2 \approx \lambda_{0.5}(1 + 0.5\alpha L\lambda_{0.5}/K_0)$ , and the full width at half maximum (FWHM) of electro-optic coupling is about

$$\Delta\lambda = \lambda_2 - \lambda_1 \approx \varepsilon\lambda_{0.5}, \quad (3)$$

where  $\varepsilon = |\alpha L|/K_0$ . Obviously, one can increase the bandwidth by increasing  $\varepsilon$ . For instance, when  $\varepsilon = 0.01 \sim 0.1$ ,  $\lambda_{0.5} = 1550\text{nm}$ , then  $\Delta\lambda \approx 15.5 \sim 155\text{nm}$ . If one wants to obtain a broadband quasi-phase matched electro-optic coupling from  $\lambda_1$  to  $\lambda_2$ , he can let

$$K_0 = -\Delta k(\lambda_1), \quad K_0 - \alpha L = -\Delta k(\lambda_2), \quad \alpha L = \Delta k(\lambda_2) - \Delta k(\lambda_1). \quad (4)$$

Then, from Eq. (4), he can get the proper parameters  $K_0$  and  $\alpha L$  for the LCPLN.

One sees from Eqs. (1) that, when the chirp coefficient is small enough so that the LCPLN can be taken as a PPLN,  $|\kappa|L = \pi/2$ , which is just the condition for the strongest coupling. Generally, it is not an easy task to qualitatively solve the equations. We notice that the Eqs. (1) are linear coupling equations, which are much similar with the equations of two-level quantum system discussed by Landau and Zener [17,18]. Without losing generality, we consider the incident light is an o-ray, i.e.,  $A_1(0) = 1$ ,  $A_2(0) = 0$ . Then the conversion efficiency from o- to e-ray is  $\eta = |A_2(L)|^2$ . By the way similar to Ref [18], one can further find

$$\eta = 1 - \exp\left(-\frac{2\pi|\kappa|^2}{|\alpha|}\right), \quad (\sqrt{|\alpha|}L \rightarrow \infty). \quad (5)$$

It should be pointed out that Eq. (5) is an asymptotic result when the crystal length  $\sqrt{|\alpha|}L$  of LCPLN is infinite. For the case of finite length of LCPLN, the conversion efficiency can also be described approximatively by Eq. (5) as long as  $\sqrt{|\alpha|}L \gg 1$ . From Eq. (5), one can get  $|\kappa|/\sqrt{|\alpha|} = [-\ln(1-\eta)/(2\pi)]^{1/2}$ , which is independent of  $\sqrt{|\alpha|}L$ . Here, for high

conversion, we set  $\eta = 0.99$ , then  $|\kappa|/\sqrt{|\alpha|} = 0.8561$ , which can be taken as the condition for perfect conversion. We choose  $\eta = 0.99$  since in this case the electro-optic coupling requires only a rather smaller  $|\kappa|/\sqrt{|\alpha|}$ . To show these, here we give some numerical results. The relation of  $|\kappa|/\sqrt{|\alpha|}$  vs.  $\sqrt{|\alpha|}L$  for different conversion from o- to e-ray are shown in Fig. 1. One sees from Fig. 1(a), when  $\sqrt{|\alpha|}L \leq 1$ ,  $|\kappa|/\sqrt{|\alpha|}$  is inversely proportional to  $\sqrt{|\alpha|}L$  for 100% conversion. For example, for 100% conversion and when  $\sqrt{|\alpha|}L = 0.01, 0.1, 1$ ,  $|\kappa|/\sqrt{|\alpha|} = 157, 15.7, 1.57$ ; that means  $|\kappa|/\sqrt{|\alpha|} \times \sqrt{|\alpha|}L = |\kappa|L = \pi/2$ , which behaves very like the case of PPLN. In contrast, when  $\sqrt{|\alpha|}L$  is large enough ( $> = 10$ ), the conversion efficiency is almost independent of  $\sqrt{|\alpha|}L$ . For this case, we find that when  $|\kappa|/\sqrt{|\alpha|}$  is at 0.86, the conversion can be as high as 99% [Fig. 1(c)], which are agreement with the above analyses. In the following, we will focus mainly on the case of larger  $\sqrt{|\alpha|}L$  ( $\sim 10$ ), and calculate the electric field for 99% conversion from equation  $|\kappa|/\sqrt{|\alpha|} = 0.8561$ , i.e.,  $E_y = 0.4281\lambda_0\sqrt{|\alpha|}[(n_o n_e)^{3/2} r_{51}]^{-1}$ .

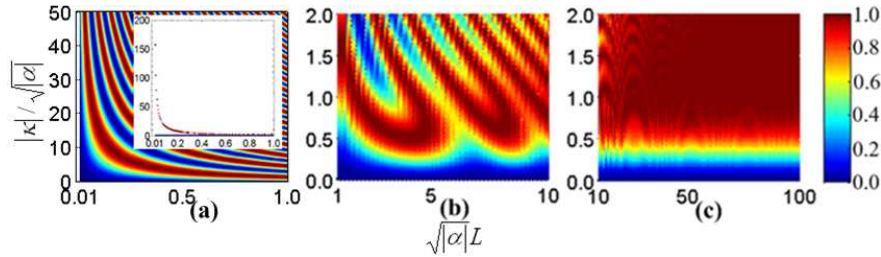


Fig. 1.  $|\kappa|/\sqrt{|\alpha|}$  vs.  $\sqrt{|\alpha|}L$  for different conversion efficiency from o- to e-ray. The incident light is o-ray, and the wavelength has a perfect phase matching point at  $0.5\sqrt{|\alpha|}L$ . The insert in (a) is a curve for 100% conversion.

### 3. Applications

In simulation, the incident light is assumed to be an o-ray, i.e.,  $A_1(0) = 1, A_2(0) = 0$ . The Sellmeier equations of LiNbO<sub>3</sub> used are from Ref [19]. And the electro-optic coefficients of LiNbO<sub>3</sub> are  $r_{51} = 28 \text{ pm/V}$ ,  $r_{22} = 3.4 \text{ pm/V}$  [15]. The temperature is set at  $T = 298 \text{ K}$ .

#### 3.1 LCPLN with duty cycle of 0.5

Now we take an example of electro-optic coupling covering 40nm of C band (1528~1568nm) in ITU DWDM specification [20]. As mentioned above, the LCPLN can be designed as follows: Let  $K_0 = |\Delta k(1528)|$ ,  $K_0 - \alpha L = |\Delta k(1568)|$ , then we have  $K_0 = 0.3110 \mu\text{m}^{-1}$ ,  $\alpha L = 0.0088 \mu\text{m}^{-1}$ ; while the length of LCPLN is chosen to be 2cm, then  $\alpha = 4.4 \times 10^{-7} \mu\text{m}^{-2}$ . From  $|\kappa|/\sqrt{|\alpha|} = 0.8561$ , we get  $E_y = 1.52 \text{ kV/mm}$  for the center wavelength 1548nm. With these conditions, we get the conversion efficiency of o- to e-ray as a function of wavelength, shown in Fig. 2(a), where the FWHM is 40nm, from 1528 to 1568nm, which agrees well with

the expectation. Similarly, we make the calculations for the LCPLNs with lengths 3, 4, 5cm, respectively. The results are shown in Fig. 2(b), 2(c) and 2(d), which indicate that, for the same bandwidth, as the length of LCPLN increases,  $\alpha$  and  $E_y$  will decrease. In fact, the bandwidth of LCPLN is not limited to be 40nm. Figure 3 shows the conversion efficiency of several LCPLNs that cover 20nm, 80nm, 120nm. By Similar way, one can also obtain the bandwidth larger than 120nm by choosing a larger  $\varepsilon(\propto |\alpha|)$ . However, a larger coefficient means a larger  $E_y$  ( $E_y \propto \sqrt{|\alpha|}$ ), which should be considered in practical use.

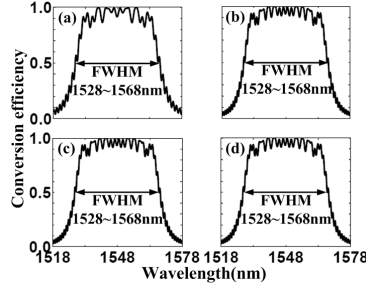


Fig. 2. Numerical simulations of electro-optic coupling covering 40nm in LCPLNs with different lengths. (a) 2cm,  $\alpha = 4.4 \times 10^{-7} \mu\text{m}^{-2}$ ,  $E_y = 1.52\text{kV/mm}$ ; (b) 3cm,  $\alpha = 2.9 \times 10^{-7} \mu\text{m}^{-2}$ ,  $E_y = 1.24\text{kV/mm}$ ; (c) 4cm,  $\alpha = 2.2 \times 10^{-7} \mu\text{m}^{-2}$ ,  $E_y = 1.08\text{kV/mm}$ ; (d) 5cm,  $\alpha = 1.8 \times 10^{-7} \mu\text{m}^{-2}$ ,  $E_y = 0.96\text{kV/mm}$ .

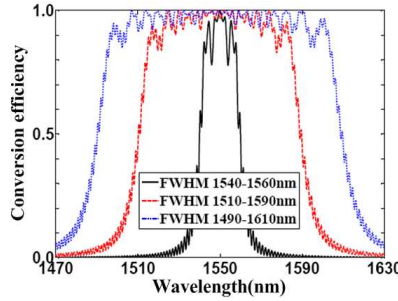


Fig. 3. Numerical simulations of conversion efficiency of broadband electro-optic coupling in LCPLN with FWHM 20nm, 80nm and 120nm, respectively. The length of LCPLN is 2cm. Solid line: 1540-1560nm; dash line: 1510-1590nm; dotted line: 1490-1610nm.

### 3.2 LCPLN with changing duty cycle-Ripples reduction

For practical use, the ripples reduction of the conversion efficiency is important. One can reduce the ripples by changing the duty cycle of LCPLN, called apodization [21,22]. Several apodization profiles can be used. Here we use the tanh profile. The Fourier coefficients and the duty cycles corresponding to tanh profile are

$$f_0(x) = 2D(x) - 1, \quad f_1(x) = \frac{1}{i\pi} \left\{ 1 - \cos[2\pi D(x)] + i \sin[2\pi D(x)] \right\}, \quad (6a)$$

$$D(x) = \frac{1}{2} \tanh\left(\frac{2ax}{L}\right) \left(0 \leq x < \frac{L}{2}\right), \quad D(x) = \frac{1}{2} \tanh\left[\frac{2a(L-x)}{L}\right] \left(\frac{L}{2} \leq x \leq L\right), \quad (6b)$$

where  $a$  is an apodization parameter and is set at 3. Figure 4 shows the  $|f_1(x)|$  corresponding respectively to unapodized LCPLN and apodized LCPLN with tanh profile. One can see that the curve of tanh profile has a FWHM of 0.88. As well known, the coupling coefficient  $|\kappa(x)|$  is proportional to  $|f_1(x)|$ . Therefore, the FWHM of apodized LCPLN will decrease to about 0.88 for a unapodized LCPLN. That is, Eqs. (3) and (4) should be modified as:

$$\Delta\lambda \approx \gamma\epsilon\lambda_{0.5}, \quad (7a)$$

$$K_0 - \frac{1}{2}(1-\gamma)\alpha L = -\Delta k(\lambda_1), \quad K_0 - \frac{1}{2}(1+\gamma)\alpha L = -\Delta k(\lambda_2), \quad \gamma\alpha L = \Delta k(\lambda_2) - \Delta k(\lambda_1), \quad (7b)$$

where  $\gamma = 0.88$  for the apodized LCPLN with tanh profile ( $a = 3$ ). Figure 5 shows the ripples reduction with apodized LCPLN, where the bandwidths designed are 20 (1540-1560), 40 (1528-1568), 80 (1510-1590) and 120nm (1490-1610nm), respectively and the lengths of LCPLN are set as 2cm. It should be noticed that the parameters of the crystals are now obtained from Eq. (7b) than from Eq. (4). One sees that the ripples are effectively reduced by using apodized LCPLN- the tops of the conversion efficiency curves become much flat. And the FWHMs, however, become 16, 36, 76 and 116nm, respectively, slightly smaller than those of design. The apodized  $\chi^{(2)}$  grating has been experimentally reported [22], meaning the fabrication of such grating is feasible. But there exists a limitation to the smallest duty cycle. For example, the domain width of 0.5  $\mu\text{m}$  or less is hard to fabricate [21].

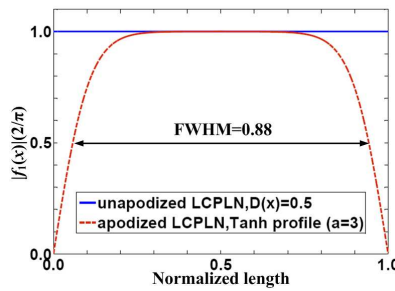


Fig. 4.  $|f_1(x)|$  corresponding respectively to unapodized LCPLN ( $D(x) = 0.5$ ) and an apodized LCPLN with tanh profile ( $a = 3$ ).

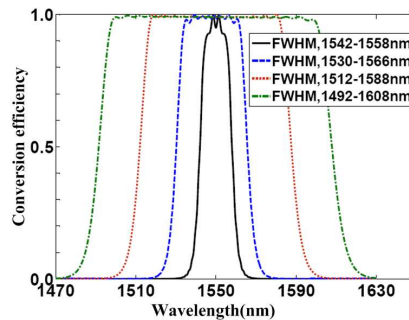


Fig. 5. Ripples reduction by using the apodized LCPLNs with tanh profile ( $a = 3$ ).

The electro-optic coupling in LCPLN with wide wavelength range would be useful for some devices, such as broadband electro-optic polarization converters and bandpass filters. For example, when the LCPLN is inserted into the interspace of two polarizers ( $y$ - and  $z$ -polarized), then the device can work as a broadband Solc-type bandpass filter in optical communication range. The Solc-type bandpass filters in LCPLN is similar to that with temperature-gradient-control technique [23] but can work much faster.

#### **4. Summary**

In summary, we have investigated electro-optic coupling of wide wavelength range in LCPLN, whose bandwidth can reach 120nm or even larger. The way to get the parameters for a desired LCPLN and the method to reduce the ripples of the conversion efficiency are shown. On it one kind of broadband Solc-type bandpass filter in optical communication range is proposed.

#### **Acknowledgements**

The authors greatly acknowledge the financial support from the National Natural Science Foundation of China (Grant No. 10874251).